Supporting Information for

Ultra-broadband Photon Harvesting in Large-area Few-Layer MoS_2 Nanostripe gratings

Mukul Bhatnagar,‡[a] Maria Caterina Giordano,‡[a] Carlo Mennucci,[a] Debasree Chowdhury,[a]

Andrea Mazzanti,[b] Giuseppe Della Valle,*[b] Christian Martella,[c] Pinaka Pani Tummala,[c]

Alessio Lamperti,[c] Alessandro Molle,[c] Francesco Buatier de Mongeot*[a]

[a] Dipartimento di Fisica, Università di Genova, Via Dodecaneso 33, 16146 Genova, Italy
Email: buatier@fisica.unige.it

[b] Dipartimento di Fisica and IFN-CNR, Politecnico di Milano, Piazza Leonardo da Vinci, 32 - 20133 Milano, Italy
Email: giuseppe.dellavalle@polimi.it

[c] CNR-IMM Unit of Agrate Brianza, via C. Olivetti 2, Agrate Brianza, I-20864, Italy

‡ These authors contributed equally.

Fabrication of MoS_2 nanostripes

The schematic shows the fabrication steps for growth of large area MoS_2 nanostripes on transparent silica substrates.

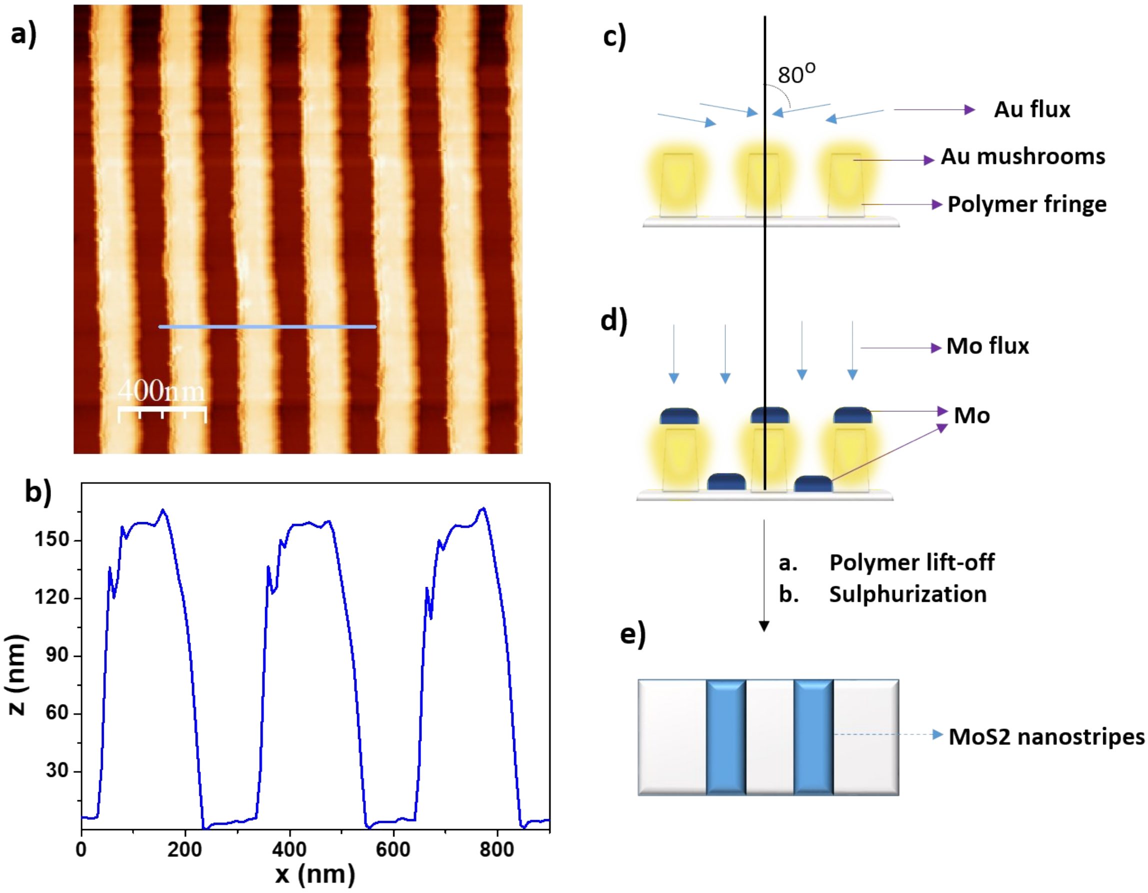

Fig. S1. Fabrication steps for large area growth of MoS_2 nanostripes. (a) Atomic force microscope (AFM) image of a polymer pattern developed on a silica substrate through LIL. (b) AFM cross-section profile of the pattern shown in panel a. (c) Polymeric mask nanopattern coated with Au nanostructures deposited at glancing angle. (d) Few-layer Mo film deposited at normal incidence on the Au coated polymeric template by sputtering deposition. (e) Laterally disconnected MoS_2 nanostripes obtained after chemical lift-off of the polymeric mask and following sulphurization at 850 °C in a sulphur enriched atmosphere.

Table S1. LIL parameters employed for the nanofabrication of the polymeric pattern in sample 1 and sample 2, respectively.

Sample	**AZ701 MR :AZ EBR**	**Dilution time (min)**	**Laser Exposure time (sec)**	**Laser Power (mw)**	**Dose**	**Development time (sec)**
1	1:2	15	30	0.473	14.19	7
2	1:3	15	35	0.479	16.76	25

Far-field Optical Spectroscopy

Optical transmission spectra of MoS_2 nanostripe arrays and of the reference flat MoS_2 film are shown in Figure 2-1 for longitudinal (TE) and transversal (TM) polarization of the incident light.

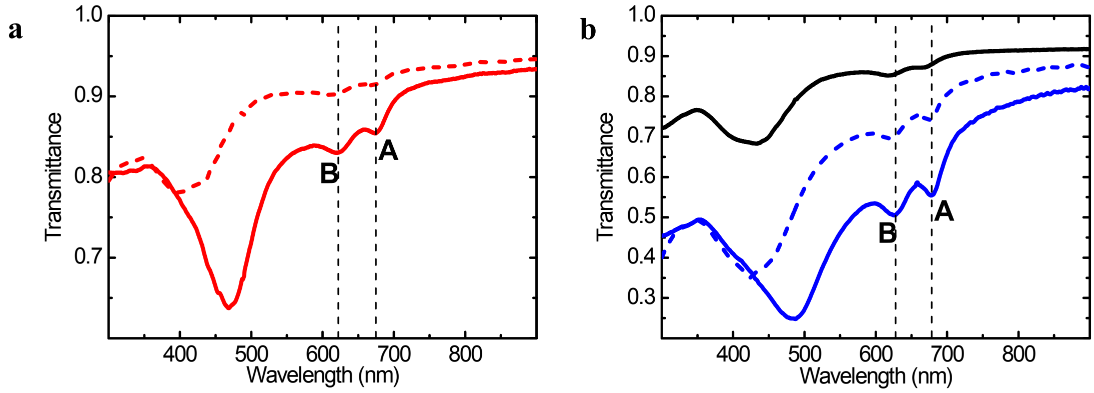

Fig. S2-1. Optical transmittance from MoS_2 nanostripes. (a) Optical transmittance from sample 1 (TE: continuous line, TM: dashed line). (b) sample 2 (TE: solid line, TM: dashed blue) and a 4 nm 2D MoS_2 flat film (continuous black).

The in-plane light scattering induced by few-layer MoS_2 nanostripe arrays has been directly measured by a custom optical setup able to detect the in-plane waveguided optical intensity (Fig. S2-2).

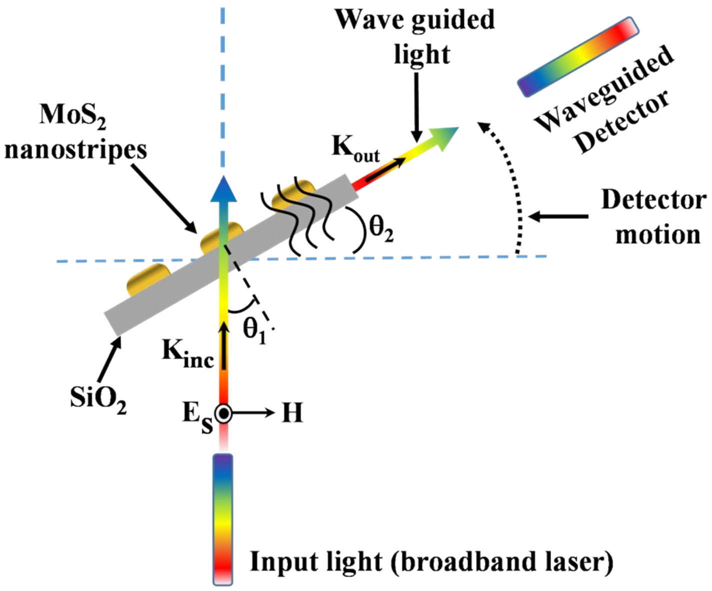

Fig. S2-2. Layout of the spectroscopic detection of in plane scattered and waveguided radiation**.** Layout of the experimental configuration employed for measuring waveguided light which exits from the side facets of the silica substrate, tangent to the substrate (experimental spectra shown in Figure 3d). Collimated illumination of the substrate takes place in s-polarization at incidence angle θ_1 with respect to the surface normal. As illumination source we employ an NKT Photonics broadband white laser (SuperK COMPACT) providing a spectrum extending from 450 nm to the NIR spectral range. The detector axis, mounted on a precision goniometer, is tilted so to collect collimated light which exits tangent to the substrate at an angle $\theta_2 = \theta_1$. The output of the detector collimating lens was coupled to the pc controlled HR4000, Ocean Optics spectrometer through an optical fiber (core diameter 600 μm). Figure 3d highlights in a straightforward way that the very thick (700 μm) substrate, acts as a low quality highly multimodal cavity, coupled to the MoS2 grating which is the flat-optics active element responsible for both launching the spectrally narrow Guided Mode Anomaly(GMA) and for coupling via scattering broadband radiation. The two mechanisms are jointly responsible for the resonant narrowband and nonresonant broadband absorption enhancement observed in our samples.

In order to evaluate the extinction signal of the A and B excitons optical transmission (extinction) spectra of Fig. 2-1 (Fig.2), have been exploited. In particular we calculated the exciton intensity as the integral of the transmission minima (extinction maxima), previously isolated from the optical background. The curves was fitted under the assumption of a Lorentzian line profile centered at 675 nm and 625 nm wavelength respectively (Fig. S2-3)

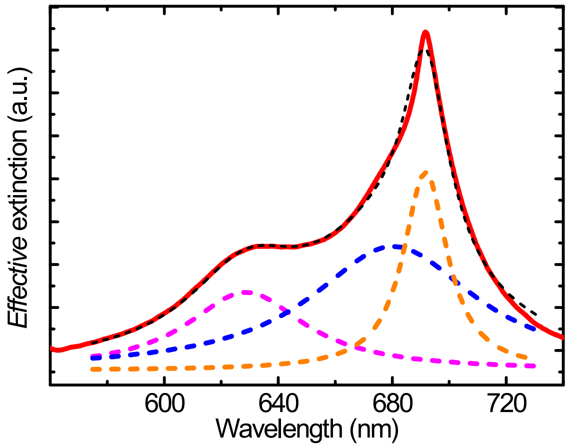

Fig. S2-3. Peak fit to the extinction spectrum. Fit profile to the measured extinction spectra at angle of incidence 75º for sample 2. Color scheme: continuous red: experimental data, dashed black: cumulative fit, dashed blue: A exciton, dashed magenta: B exciton, dashed orange: guided mode anomaly.

Absorption Numerical Modeling

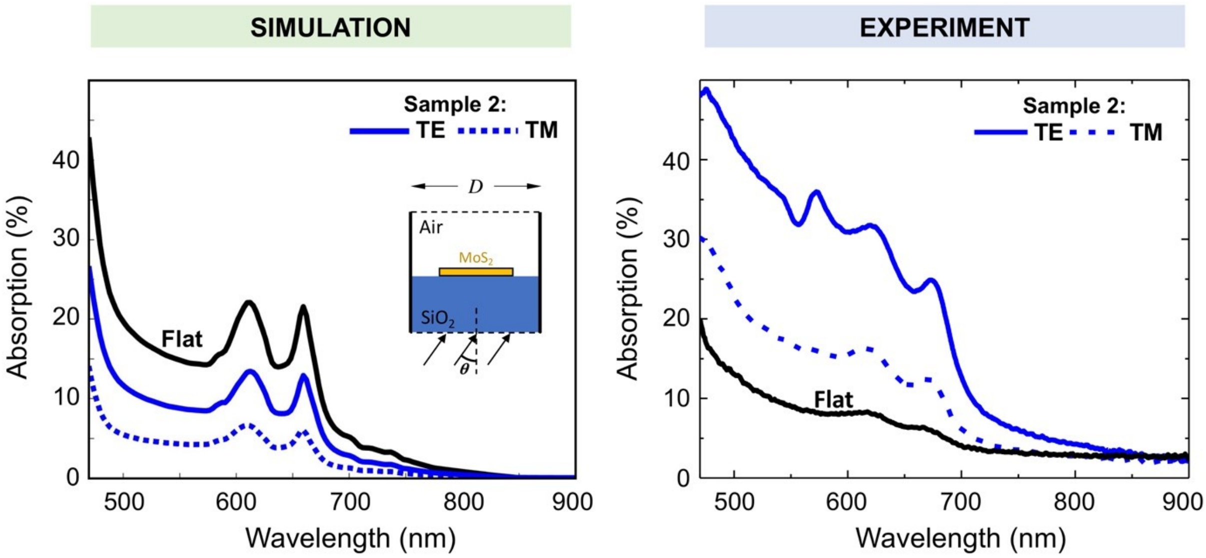

Fig. S3. Numerical simulation of absorption in sample 2 assuming an infinite substrate. (a) Numerical simulations of the absorption in sample 2 for the same excitation conditions detailed in the experiment of Fig. 4a, i.e. $\theta = 35°$ angle of incidence and TE or TM polarization, are compared with absorption simulations from a flat nanosheet of the same thickness. Differently to the simulations of Fig. 2b, an increased thickness (6 nm instead of 4 nm) for the MoS_2 layer was assumed in order to make our estimation of Mie resonant effects more conservative. The port boundary condition on the lower edge of the integration domain (inset in panel a) results into an infinite thickness of the SiO_2 substrate in the vertical direction. This assumption rules out any possible contribution from guiding effects in the substrate. (b) Experimental data from Fig. 4a is shown for better comparison.